Atmos. Meas. Tech. Discuss., 2, 1419–1452, 2009
www.atmos-meas-tech-discuss.net/2/1419/2009/

Atmospheric Measurement Techniques Discussions

Atmospheric Measurement Techniques Discussions is the access reviewed discussion forum of *Atmospheric Measurement Techniques*

Use of O_2 airglow for calibrating direct atomic oxygen measurements from sounding rockets

J. Hedin, J. Gumbel, J. Stegman, and G. Witt

Department of Meteorology, Stockholm University, 10691 Stockholm, Sweden

Received: 12 May 2009 – Accepted: 4 June 2009 – Published: 15 June 2009

Correspondence to: J. Hedin (jonash@misu.su.se)

Published by Copernicus Publications on behalf of the European Geosciences Union.

Abstract

Accurate knowledge about the distribution of atomic oxygen is crucial for many studies of the mesosphere and lower thermosphere. Direct measurements of atomic oxygen by the resonance fluorescence technique at 130 nm have been made from many sounding rocket payloads in the past. This measurement technique yields atomic oxygen profiles with good sensitivity and altitude resolution. However, accuracy is a problem as calibration and aerodynamics make the quantitative analysis challenging. In general, accuracies better than a factor 2 are not to be expected from direct atomic oxygen measurements. As an example, we present results from the NLTE (non local thermodynamic equilibrium) sounding rocket campaign at Esrange, Sweden, in 1998, with simultaneous O_2 airglow and O resonance fluorescence measurements. O number densities are found to be consistent with the nightglow analysis, but only within the uncertainty limits of the resonance fluorescence technique. Based on these results, we here describe how better atomic oxygen number densities can be obtained by calibrating direct techniques with complementary airglow photometer measurements and detailed aerodynamic analysis. Night-time direct O measurements can be complemented by photometric detection of the O_2 ($b^1\Sigma_g^+$-$X^3\Sigma_g^-$) atmospheric band at 762 nm, while during daytime the O_2 ($a^1\Delta_g$-$X^3\Sigma_g^-$) infrared atmospheric band at 1.27 µm can be used. The combination of a photometer and a rather simple resonance fluorescence probe can provide atomic oxygen profiles with both good accuracy and good height resolution.

1 Introduction

Atomic oxygen is the major carrier of chemical energy in the Earth's mesosphere and lower thermosphere (MLT) and is thus a key component for the aeronomy of this region. It is formed by O_2 photolysis mainly in the Schumann-Runge continuum and Schumann-Runge bands in the thermosphere and mesosphere, respectively, and at

AMTD

2, 1419–1452, 2009

lower altitudes in the Herzberg continuum (Brasseur and Solomon, 1984). In the mesosphere the local abundance of atomic oxygen is governed by chemical control through the O_x and HO_x cycles. Here the lifetime of O is of the order of hours because of the relatively high molecular collision and reaction rates in this denser part of the upper atmosphere. In the thermosphere the chemical lifetime of O is long (months, even years) and the local abundance is governed by dynamic control. Here O can be transported horizontally or vertically and the deposition of the stored chemical energy can take place at large spatial or temporal distances from the sources (Rees and Fuller-Rowell, 1988). Around the mesopause, in-between these two regions, the chemical and transport lifetimes are of similar magnitude and the local abundance depends on the interplay of the different control mechanisms. The transport processes involved in redistributing O in the mesopause region are long-distance transport by the global meridional circulation with ascending and descending motion in summer and winter, respectively, variations due to tidal and wave motions on various scales, as well as exchange by turbulent diffusion (Shepherd et al., 2005; Russell et al., 2005).

Accurate knowledge about the vertical distribution of O is crucial for any comprehensive study of chemical and dynamical processes in the MLT region. Measurements need to be both accurate and of good height resolution. Absolute profiles of atomic oxygen have been obtained in situ by means of rocket-borne experiments since the early 1960s. In the beginning, mass spectrometry was the dominant method but since the early 1970s the resonance fluorescence technique using the O (^{3}S-^{3}P) transition at 130 nm has taken over this role and is the only technique in use today (Dickinson et al., 1980; Sharp, 1991). Much debate has been going on about the reliability of in situ measurements by means of rocket-borne techniques (Gumbel, 1999). The existing measurements reported by different research groups show consistency in the general shape of the profiles, but little consistency in the absolute densities. The variability in the measurements is thought to be mostly of instrumental nature and not necessarily geophysical (e.g. Offermann et al., 1981). Major challenges to a quantitative analysis are the calibration and aerodynamics of the experiments. It is therefore desirable to

AMTD
2, 1419–1452, 2009

define complementary calibration procedures that are independent of the instrument characteristics of the specific direct O measurement. In this paper, we discuss such calibration procedures in terms of photometric airglow measurements.

In the mesopause region the recombination of atomic oxygen generates molecular oxygen in a number of metastable states. Through a number of energy transfer and quenching processes the excited O_2 then gives rise to nightglow emissions covering the spectral range from the ultraviolet to the infrared (Meriwether, 1989; Wayne, 2000). These processes cause a complex and strongly altitude dependent photochemistry between about 85 and 105 km. Also energy transfer to atomic oxygen (Barth and Hildebrandt, 1961) and reactions between ozone and hydrogen forming vibrationally excited OH molecules (Bates and Nicolet, 1950) contribute to the nightglow emissions with different peak altitudes depending on the details of the photochemistry.

It is generally accepted that the excitation energy originates from the recombination of O, but it took long time to establish the exact mechanisms and reaction rates, and some have still not been established. There have been several rocket experiments in the past with the objective to simultaneously study atomic oxygen density and oxygen airglow intensity (e.g. Thomas, 1981; Sharp, 1980; McDade et al., 1984). However the most extensive of these multi-instrumented rocket studies was the set of campaigns with OXYGEN/S35 in March 1981 (Witt et al., 1984) followed by the ETON (Energy Transfer in the Oxygen Nightglow) venture conducted in March 1982 from South Uist, UK (Greer et al., 1986) and OASIS (Oxygen Atom Studies in Space) conducted from White Sands in June 1983 (Murtagh et al., 1990). The ETON campaign was a multi-rocket campaign in which a series of seven payloads was launched to measure altitude profiles of emission features and atmospheric composition. The analysis of the ETON database resulted in detailed knowledge about nightglow excitation and quenching mechanisms (Greer et al., 1986; McDade et al., 1986a, b; 1987a, b; Murtagh et al., 1986), and a numerical model has been developed based on this (Murtagh, 1989; Murtagh et al., 1990).

The plan for this paper is to first present results on the O_2 nightglow and direct atomic

AMTD
2, 1419–1452, 2009

oxygen measurements obtained during the NLTE rocket campaign. In the discussion in Sect. 3 the inverted nightglow emissions are compared to the direct O measurements and also comparisons to other measurements are made. We conclude in Sect. 4 with a discussion of the reliability of O number densities retrieved from the resonance fluorescence technique and the possibility to improve these by calibration with simultaneous O_2 nightglow or dayglow measurements.

2 NLTE – techniques and results

The Swedish-led NLTE (non local thermodynamic equilibrium) sounding rocket campaign was conducted at the Esrange rocket range near Kiruna in northern Sweden in March 1998. It was an international rocket campaign (involving also groups from Norway, Germany, Austria and the USA) with the prime purpose to investigate processes contributing to the energy balance of the MLT region during polar winter. Rocket-borne and ground-based measurements investigated dynamic conditions and the distribution of neutral and charged species between 70 and 130 km.

The central aim of the Stockholm group was the study of processes controlling the distribution of atomic oxygen. This was done by directly measuring atomic oxygen using the resonance fluorescence and absorption technique simultaneously with photometric measurements of the O_2 atmospheric band at 762 nm and the N_2^+ (0-0) 1st negative band at 391 nm. The O_2 atmospheric band is a product of O atom recombination and can be used as an alternative way to retrieve atomic oxygen densities. The N_2^+ (0-0) 1st Negative band is a sensitive indicator for the presence of precipitating (auroral) electrons. In addition, the passband of the N_2^+ photometer comprises the (5-3) band of the O_2 Chamberlain system, which also is a result of atomic oxygen recombination. Additional experiments on the NLTE payloads addressed temperature, neutral and plasma densities as well as turbulence (Lübken et al., 1999; Friedrich et al., 1999). By obtaining profiles of total density, absolute O densities can be converted into mixing ratios, which helps to distinguish dynamic and chemical influences on the O

AMTD
2, 1419–1452, 2009

distribution.

Two identical rocket payloads were launched as the main events during the campaign. NLTE-1 was launched on 3 March at 22:33 UT and NLTE-2 three days later on 6 March at 21:26 UT into geomagnetically very quiet and extremely quiet conditions, respectively. On NLTE-2 the 391 nm photometer showed no sign of electron precipitation thus ensuring a study of the atmospheric energetics and chemistry in the absence of auroral influence. In addition, this made it possible to study the weak O_2 Chamberlain emission in the 391 nm filter band. The electron density measurement onboard the payload (Langmuir probe calibrated by a radio wave propagation experiment (Jacobsen and Friedrich, 1979) showed very low concentrations (see Fig. 1) and the ground-based O(^{1}S) Green Line photometer showed weak emissions of 250 and 120 R during the first and second launch, respectively (R (Rayleigh) is a common unit for airglow and auroral emissions and equals $4\times\pi\times10^{-6}\times L$, where L is the radiance in units of photons s^{-1} str^{-1} cm^{-2}). The a_p index of geomagnetic activity showed low, but not extremely low, values of 3 and 5 during the first and second launch, respectively.

2.1 Resonance fluorescence and absorption

The resonance fluorescence technique is based on the resonance transition of O ($^3S_1$-$^3P_{2,1,0}$) at 130.4 nm. This triplet is emitted using an oxygen discharge lamp and the radiation can be resonantly absorbed and scattered by O atoms in the vicinity of the instrument. A suitable detector collects part of this scattered light as a direct measure of the atomic oxygen abundance. The use of the resonance transition at 130.4 nm to measure atomic oxygen in the atmosphere was originally proposed by R. A. Young (1961). For a detailed description of this measurement technique see e.g. Dickinson et al. (1980), Sharp (1991), or Gumbel et al. (1998). Atomic species are particularly suitable for optical measurement techniques because of their large absorption cross section at resonance frequencies. The O ($^3S_1$-$^3P_{2,1,0}$) absorption cross section of about 2×10^{-13} cm^{-2} exceeds the Rayleigh scattering cross section by 11 orders of

AMTD
2, 1419–1452, 2009

magnitude and the absorption cross section of molecular oxygen by 6 orders of magnitude. Thus this technique provides both a sensitive and selective measurement of the atmospheric atomic oxygen abundance.

2.1.1 Calibration

The resonance fluorescence measurement represents a very sensitive but not very accurate measurement as it is not easy to calibrate. The relationship between the fluorescence signal and the atmospheric O density is determined by the intensity and emission line shapes of the lamp, detector sensitivity, measurement geometry, atmospheric temperature and aerodynamic flow properties in the measurement volume. Different calibration techniques exist and include numerical (e.g. Ulwick et al., 1994; Gumbel and Witt, 1997), laboratory (e.g. Sharp, 1991) and in situ absorption methods (e.g. Dickinson et al., 1980; Gumbel et al., 1998). Knowledge about the line shapes of the lamp's resonance emission is essential for all three calibration techniques, and indirect information of the line shapes can be obtained from curve-of-growth measurements (e.g. Rawlins and Kaufman, 1977). The only direct measurement of resolved lamp emission line shapes have been reported by Jenkins et al. (1985).

For NLTE in situ absorption calibrations, supported by numerical simulations, were utilised in a similar way as described by Gumbel et al. (1998) for an earlier rocket measurement. The in situ absorption measurement, as described by e.g. Dickinson et al. (1980) and Gumbel et al. (1998), on the other hand, is independent of absolute instrument parameters as it presents a relative measurement and thus provides a direct way of calibrating the atmospheric data. On NLTE, booms were deployed near the top of the payload positioning absorption detectors opposite the O lamp, at distances of 33 and 65 cm, to measure the relative amount of the 130.4 nm triplet transmitted by the oxygen atoms. Although improving the measurement accuracy, the absorption calibration is intrinsically uncertain since the absorption process is very sensitive to the relationship between atmospheric absorption line shapes and emitted lamp line shapes (Gumbel and Witt, 1997). While the former is essentially determined by Doppler broad-

ening at the atmospheric temperature, the latter is only known with limited accuracy. Our NLTE analysis is based on the line shape results reported by Jenkins et al. (1985) from laboratory measurements with various lamp parameters. The stability of the lamp output before and during flight is an additional source of uncertainty. In total, we estimate the overall uncertainty of the direct atomic oxygen measurements during NLTE to be a factor of 2–3, in consistency with earlier investigations of the resonance fluorescence and absorption technique (Gumbel, 1999).

2.1.2 Aerodynamics

For almost all rocket-borne measurements, also aerodynamic effects have to be considered very carefully. As the payload moves through the atmospheric region of interest, conditions change from continuum flow via the transition regime to free molecular flow. The high velocity of the rocket payload can produce many different perturbations related to aerodynamics. These include compression and rarefaction of the atmospheric density, composition changes due to mass-dependent species separation, chemical reactions in the shock region and on payload surfaces, excitation of atoms and molecules (i.e. payload glow), Doppler influence on optical measurements, and contamination of the measurement volume by outgassing and desorption from the payload itself. A discussion of atomic oxygen measurements from sounding rockets under such flow conditions has been given by Bird (1988). For studying the aerodynamic effects in these changing flow conditions we use the DSMC (Direct Simulation Monte Carlo) model DS2V v.4.5 (Bird, 1994). With this model we can simulate two-dimensional and axially symmetric problems from continuum flow conditions to free molecular flow.

In Fig. 2a, c the simulated number density field around the NLTE payload is shown for two different altitudes. Figure 2b, d shows the O mixing ratio normalised to the undisturbed O mixing ratio in the flow field. The deployed absorption boom in the plots indicates the position of the absorption path. At 90 km altitude (Fig. 2a, b) there is a very pronounced shock region around the payload and the absorption detector

is positioned outside the disturbed region. In panel (b) it can be seen that there is a depletion of O close to the payload but an increase further out at the edge of the shock region. This aerodynamic separation effect is caused by the lower mass of the O atom with respect to the N_2 and O_2 molecules. At 120 km (Fig. 2c, d) the shock region is smoothed out and the absorption detector is well inside the disturbed region. Panel d shows here a depletion of O relative to the undisturbed atmosphere along the entire absorption path.

Figure 3 shows the mean relative change of the total air density and the O density in the absorption path for different altitudes from 80 to 125 km. During the ascent of the payload, the air density is higher in the measurement region than in the undisturbed atmosphere. Without correction, the measurements will overestimate the O density. It is however not sufficient to investigate only the total air density. Rather, the additional effect on the mixing ratio of the O atoms needs to be included. For the NLTE measurements, the O mixing ratio in the absorption path up to 95 km is slightly higher than in the surrounding atmosphere, whereas above this altitude the fraction is significantly lower. The reason is that at the lower altitudes the detector is outside the shock region and the absorption path includes both the depleted region near the payload and the O-enriched region near the outer edge of the shock. Above 95 km the shock grows and the entire absorption path is inside the perturbed region with depleted O.

The velocity of the payload and the temperature in the perturbed region are not high enough for chemical reactions, or excitation of atoms and molecules. Neither are Doppler influences on the resonance measurement significant as the absorption path is largely perpendicular to the payload velocity vector. Contamination of the measurement volume by outgassing and desorption from the payload is evident during the upleg part of the flight. Effects on O absorption measurements have been discussed by Gumbel et al. (1998).

2.1.3 Direct atomic oxygen results

The result of the O fluorescence measurement during NLTE-2 is shown in Fig. 4. This profile has been calibrated with the absorption measurement and corrected for aerodynamic effects as described in the two previous sections. The measurement shows a structured profile with a peak density of 2.7×10^{11} atoms per cm^3 at 97.5 km and a very sharp cut-off at the lower ledge below 90 km. A comparison to the NLTE-1 results will be given in Sect. 3.

2.2 Nightglow photometry

The molecular oxygen band systems are, together with the O (^{1}S-^{1}D) Green Line and the OH Meinel band system, the main contributors to the terrestrial nightglow spectrum. As mentioned earlier, atomic oxygen is mainly formed through O_2 photolysis during the day and can then recombine to form excited oxygen molecules during the night. The recombination reaction has an exothermicity of 5.12 eV which mainly resides in the newly formed O_2 molecule, the so called precursor state of the molecular and atomic oxygen nightglow emissions. With this available energy high vibrational levels of the ground state ($X^3\Sigma_g^-$) or any of the five bound states ($a^1\Delta_g$, $b^1\Sigma_g^+$, $c^1\Sigma_u^-$, $A^3\Sigma_u^+$, $A'^3\Delta_u$) may be formed (Slanger and Copeland, 2003). The energy levels of these states are shown in Fig. 5. Another weakly bound state, $^5\prod_g$, has been proposed as a likely precursor to the above lower-lying light-emitting states. The excited oxygen molecule may then decay through emission of a photon, energy transfer to O, or quenching by other atoms or molecules (e.g. O_2, N_2, O or CO_2).

2.2.1 Nightglow measurements during NLTE

The second strongest O_2 nightglow emission feature is the atmospheric band system ($b^1\Sigma_g^+ \rightarrow X^3\Sigma_g^-$) dominated by the (0-0) and (0-1) bands at 762 nm and 864 nm, respectively. The (0-0) band can not be studied from the ground because of self absorption

AMTD
2, 1419–1452, 2009

in the atmosphere between the emitting layer and the observer. It is however easy to measure with filter photometers from sounding rockets.

Optical measurements of the upper atmosphere from sounding rockets have been made since the 1950s (Heppner and Meridith, 1958) both for understanding airglow chemistry in itself and for using airglow as a tool to understand atmospheric (e.g. dynamical) processes. For airglow measurements a filter photometer is positioned under the nose cone viewing along the rocket axis. During ascent, after the nosecone ejection, the photometer then counts the incoming photons from the overhead column. When the rocket passes through the layer the measured photon flux drops and above the emission layer only weak background emissions from the zodiacal and galactic light are present (unless there are auroral emissions in the wavelength region defined by the photometer passband). After the profile has been corrected for background emissions and attitude (van Rhijn effect) it is converted from counts to radiance using pre-flight laboratory calibrations. The profile can then be smoothed and numerically differentiated to yield the volume emission rate of the emitting layer.

The nightglow model used in the following is a numerical model based almost exclusively on the findings of the ETON rocket campaign. It is a self-consistent model of the most common nightglow emissions including the O(^{1}S) Green Line, OH Meinel and several O_2 band emissions (Murtagh, 1989; Murtagh et al., 1990). For the O_2 atmospheric band, the emitting state ($b^1\Sigma_g^+$) is assumed to be excited via an energy transfer mechanism from the precursor state with O_2 as the transfer agent (Greer et al., 1986). The volume emission rate of the O_2 atmospheric band may be expressed as (Murtagh, 1989)

$$V_{\mathrm{at}} = \frac{A_1 \cdot k_1 [\mathrm{O}]^2 \{[\mathrm{N_2}] + [\mathrm{O_2}]\} [\mathrm{O_2}]}{\left\{A_2 + k_2^{\mathrm{O_2}} [\mathrm{O_2}] + k_2^{\mathrm{N_2}} [\mathrm{N_2}] + k_2^{\mathrm{O}} [\mathrm{O}]\right\}} \cdot \frac{1}{\left\{C^{\mathrm{O_2}} [\mathrm{O_2}] + C^{\mathrm{O}} [\mathrm{O}]\right\}} \quad (1)$$

Equation (1) comprises the excitation and emission processes as well as quenching of the precursor state and $O_2(b^1\Sigma_g^+)$ by various atmospheric constituents. A_1 is the (0-0)

AMTD
2, 1419–1452, 2009

band transition probability, A_2 is the inverse radiative lifetime of $O_2(b^1\Sigma_g^+, v{=}0)$, k_1 is the temperature-dependent rate coefficient for the three-body recombination of atomic oxygen, and $k_2^{O_2}$, $k_2^{N_2}$ and k_2^{O} are the rate coefficients for the quenching of $O_2(b^1\Sigma_g^+)$ by O_2, N_2 and O and are all determined by laboratory investigations. The coefficients C^{O_2} and C^{O} represents the quenching of the precursor state and were derived empirically from the ETON measurements. The values of all coefficients can be found in Table 1. The O_2 atmospheric band profile measured during NLTE-2 is the black profile shown in Fig. 6.

The second photometer on the NLTE payloads measured the emission from the N_2^+ 1st Negative band at 391.4 nm. This emission is a sign of precipitating auroral electrons and thus a sensitive indicator of auroral activity. Included in the passband of this photometer is also the (5-3) band of the O_2 Chamberlain system ($A'^3\Delta_u \rightarrow a^1\Delta_g$) at 390.5 nm. This is not a well studied emission feature since it is very faint and easily dominated by the presence of even weak auroral emissions. Emissions from the Chamberlain band system are also in general blended in the much stronger Herzberg I and II band systems. During the NLTE-2 launch the auroral activity was extremely low and the O_2 Chamberlain band could thus be studied. The emitting state is thought to be directly produced in the three-body recombination reaction of atomic oxygen and the loss processes are quenching by O and O_2. The volume emission rate of the Chamberlain system can thus be expressed as

$$V_{ch} = \frac{\gamma \cdot A_3 \cdot k_1 [O]^2 \{[N_2] + [O_2]\}}{k_3^{O} [O] + k_3^{O_2} [O_2]} \quad (2)$$

where k_1 is again the temperature-dependent rate coefficient for the three-body recombination of atomic oxygen, and k_3^{O} and $k_3^{O_2}$ are the rate coefficients for the quenching of the emitting state by O and O_2, respectively, γ is the production efficiency of the emitting state, $O_2(A'^3\Delta_u)$, in the recombination reaction, and A_3 is the inverse of the radiative lifetime (see Table 1 for values). Chamberlain band emissions are not avail-

able from the ETON campaign, but they were measured before (Stegman et al., 1983; Stegman and Murtagh, 1991) and are included in the model. The Chamberlain profile from NLTE-2 is the gray profile shown in Fig. 6. The volume emission rate of the Chamberlain band system is about 50 times weaker than that of the atmospheric band system. The difference in peak altitudes is consistent with the photochemistry of the two emitting states where the Chamberlain band emission is directly produced in the recombination reaction without an intermediate energy transfer step, and thus radiates at higher altitudes.

2.2.2 Atomic oxygen retrievals

Equations (1) and (2) can readily be inverted to derive the atomic oxygen densities from any atmospheric band or Chamberlain emission profile using the reaction coefficients derived from the ETON measurements. A necessary input to this inversion is the temperature and neutral density of the background atmosphere. The atomic oxygen profiles derived from the NLTE-2 nightglow profiles are shown in Fig. 7. The gray line is the profile derived from the Chamberlain band emission and the thick red and black lines are the profiles derived from the atmospheric band emission with and without quenching of the emitting state by atomic oxygen, respectively (McDade et al., 1986a; Murtagh et al., 1990). The dashed red and black lines indicate the uncertainties in the inversion due to uncertainties in the reaction rates. For this analysis the atmospheric temperature and density have been taken from MSIS-E90 (Hedin, 1991) since on NLTE-2 the onboard neutral density and temperature measurement failed. It can be noted that for the night of the launch lidar measurements up to 85 km, well below the emission layer, indicate that MSIS is ~30 K too warm. Using the temperature climatology of Rauthe et al. (2008) and atmospheric density climatology of Rapp et al. (2001) the sensitivity of the nightglow inversion to atmospheric temperature and density variability can be estimated. At 95 km (close to the peak altitude of the oxygen profile) the temperature variability in March is typically ±6 K which yields a variability in the O density inversion of ±4%. At the same altitude the total density variability is typically

AMTD
2, 1419–1452, 2009

±12% for the winter months (January to March) which translates into a variability of the inverted O density of ±10%. Above ~105 km the possible errors in the measured atmospheric band emission rates are large (low signal to noise ratio) and the inversion procedure used to determine the atomic oxygen number density becomes unreliable (Murtagh et al., 1990).

The nightglow inversion yields O profiles with reliable absolute values (peak density). However, the altitude resolution is limited and the detailed structure of the derived profiles, especially from the weak Chamberlain band emission, may not be geophysical. The atmospheric band inversion indicates a double peak profile with peak atomic oxygen densities of 4.5×10^{11} cm^{-3} at 94 km and 4.4×10^{11} cm^{-3} at 99 km. The main peak from the Chamberlain band inversion yields an atomic oxygen density of 4.7×10^{11} cm^{-3} at 95 km.

3 Discussion

The atomic oxygen profiles derived from the A-band and Chamberlain emissions are in good agreement with each other when it comes to absolute peak density and altitude. Consistency is also found with the ground-based photometer measurements of the O (^{1}S→^{1}D) Green Line at 557.7 nm. The nightglow model provides a direct relationship between atmospheric band and Green Line emission rates, based on the rate coefficients from ETON. For the atmospheric band measurement from NLTE-2 the nightglow model predicts a Green Line emission of 125–130 R, which is in very good agreement with the 120–125 R seen by the ground-based Green Line photometer. However, as can be seen in Fig. 8, the atomic oxygen number density profile derived from the direct resonance fluorescence and absorption technique (dashed red line) is not consistent with the number densities derived from the nightglow emissions and differs by a factor of about 1.7 in the peak density. As discussed in Sect. 2.1, this difference is most likely due to difficulties in achieving a good calibration of the direct O measurement. It can be noted that the direct measurement of O is consistent with the nightglow analysis within

AMTD
2, 1419–1452, 2009

the uncertainty of the measurement technique. For comparison, also the O profile from the MSIS-E90 model (dashed gray line) is shown in Fig. 8.

In order to improve the uncertainty and compatibility of rocket-borne atomic oxygen measurements, we now suggest using the atmospheric band emission measurement to calibrate the direct measurement. This is best done in terms of the entire atmospheric O column and the undifferentiated photometer measurement. Starting out from the directly measured O profile from NLTE-2, using the model we first calculate the corresponding volume emission rate of the atmospheric band and then integrate this profile to obtain a column emission. This can be compared directly to the rocket-borne photometer measurements. The ratio between these two column radiances is then determined and used as a calibration factor. The atomic oxygen profile measured directly is then multiplied by the square root of this factor (since the volume emission rate is proportional to $[O]^2$, see Eq. 1). The resulting calibrated atomic oxygen profile with a peak density of 4.45×10^{11} cm^{-3} is the solid red profile in Fig. 8.

The corresponding results from the NLTE-1 flight are shown in Fig. 9 with the direct O measurement and the atmospheric band inversions. As opposed to NLTE-2, on this flight the 390 nm photometer detected a weak variable N_2^+ auroral emission and thus the O_2 Chamberlain band emission could not be retrieved. The direct measurement yielded a peak density of 5.6×10^{11} cm^{-3} at 97 km, whereas the nightglow inversion yielded a lower value. On NLTE-1 the measurement of the neutral density and temperature gave good background information for the A-band inversion. The solid blue line in Fig. 9 shows the airglow-calibrated O profile with a peak density of 4.6×10^{11} cm^{-3}. This airglow-calibrated peak value is 31% lower than obtained by the direct technique (dashed blue line), as compared to NLTE-2 where the calibrated peak value was 72% higher.

Figure 10 shows a comparison of the atomic oxygen profiles derived from the NLTE resonance fluorescence and O_2 atmospheric band measurements with other measurements. The thick lines indicate atomic oxygen profiles from resonance fluorescence measurements and the thin lines are the results from the O_2 atmospheric band inver-

AMTD
2, 1419–1452, 2009

sion. The black profiles were obtained during the SOAP/WINE (the Selective Optical Atmospheric Probe/Winter In Northern Europe, solid thick and thin lines) and USU (Utah State University, dashed line, 72 min after SOAP, resonance fluorescence only) measurements during the MAP/WINE (Middle Atmosphere Program/Winter In Northern Europe) sounding rocket campaign (Dickinson et al., 1987). The blue lines are the NLTE-1 profiles (resonance fluorescence profile without nightglow calibration) and the red lines are NLTE-2 profiles (again resonance fluorescence profile without nightglow calibration). The green profiles are from measurements during the OXYGEN/S35 sounding rocket campaign (Witt et al., 1984). Note that the resonance fluorescence measurements vary by a factor of 50 while there is only a spread by a factor of 3 in the nightglow inversion profiles.

4 Conclusions

Rocket-borne resonance fluorescence at 130.4 nm in combination with in situ absorption provides an accurate way of measuring atomic oxygen if a detailed characterisation of the instrument is available. In particular, sufficient knowledge about the O resonance lamp and its emitted line shapes is needed. This was the basis for the direct O measurements during the ETON project, comprising e.g. highly resolved laboratory studies of the lamp output. Consequently, the ETON results on atomic oxygen and nightglow rate coefficients are the best available and have come in use as a standard. This way of performing O measurements with detailed instrument calibration before flight and in-flight is the best way, but it is generally very difficult and too expensive to achieve for every single rocket flight. A simple way of calibrating atomic oxygen measurements is therefore highly desirable.

Our way of calibrating the direct O measurement with simultaneous airglow measurements, combined with a detailed aerodynamic analysis, is the second best. The airglow photometers are relatively easy to calibrate in the laboratory. In this way knowledge of the exact performance of the resonance fluorescence instrument, and expensive and

complicated absorption measurements, are not needed. Major sources of error are no longer the instrument calibration, but only the uncertainties in the airglow reaction coefficients and the background atmosphere density and temperature. Good neutral density and temperature measurements are desirable for a good analysis considering the limited ability of model atmospheres to represent the local atmospheric conditions at the time of measurement.

For daytime measurements the atmospheric band is not adequate as a calibration of O measurements because of the dominance of to high background illumination due to direct solar resonance excitation. As replacement it is possible to use the (0-0) band of the O_2 ($a^1\Delta_g \rightarrow X^3\Sigma_g^-$) IR atmospheric system at 1.27 µm (Mlynczak et al., 1993). This emission is related to the photolysis of ozone which, during the day, is in steady state with atomic oxygen (see Fig. 11) and a retrieval of atomic oxygen is thus possible. Mlynczak et al. (2001) discuss combined rocket-borne measurements of the IR-atmospheric band and the atmospheric band during daytime.

In summary, we suggest future rocket-borne measurements of atomic oxygen profiles to be based on combinations of a relatively simple "uncalibrated" 130.4 nm resonance fluorescence probe and a calibrated airglow photometer. While the resonance fluorescence probe provides the sensitivity and altitude resolution, the photometer provides the necessary calibration of the atomic oxygen data. This approach would also largely improve the compatibility between various rocket-borne O measurements as inter-comparisons between photometers are much more straight-forward than inter-comparisons between complex resonance fluorescence techniques. The airglow inversions presented in the present paper are based on nightglow rate coefficients from the ETON database. If the relevant rate coefficients are changed as a result of future investigations, a re-calibration of O profiles will be straight-forward for retrievals that are based on airglow photometry.

Acknowledgement. We thank D. P. Murtagh for providing the ETON model and M. Friedrich for the electron density data. The NLTE rocket campaign was funded by the Swedish National

Space Board. J. Hedin thanks for the support from the Swedish National Graduate School of Space Technology.

References

Barth, C. A. and Hildebrandt, A. F.: The 5577 Å airglow emission mechanism, J. Geophys. Res., 66, 985–986, 1961.

Bates, D. R. and Nicolet, M.: The photochemistry of atmospheric water vapour, J. Geophys. Res., 55, 301–327, 1950.

Bird, G. A.: Aerodynamic effects on atmospheric composition measurements from rocket space vehicles in the thermosphere, Planet. Space Sci., 36, 921–926, 1988.

Bird, G. A.: Molecular Gas Dynamics and the Direct Simulation of Gas Flows, Oxford University Press, Oxford, 1994.

Brasseur, G. and Solomon, S.: Aeronomy of the Middle Atmosphere, D. Reidel Publishing Company, Dordrecht, 1984.

Campbell, I. M. and Gray, C. N.: Rate constants for $O(^3P)$ recombination and association with $N(^4S)$, Chem. Phys. Lett., 18, 607–609, 1973.

Dickinson, P. H. G., Bain, W. C., Thomas, L., Williams, E. R., Jenkins, D. B., and Twiddy, N. D.: The determination of the atomic oxygen concentration and associated parameters in the lower ionosphere, Proc. R. Soc. Lond. A, 369, 379–408, 1980.

Dickinson, P. H. G., Witt, G., Zuber, A., Murtagh, D. P., Grossmann, K. U., Bruckelmann, H. G., Schwabbauer, P., Baker, K. D., Ullwick, J. C., and Thomas, R. J.: Measurements of odd oxygen in the polar region on 10 February 1984 during MAP/WINE, J. Atm. Terr. Phys., 49, 843–854, 1987.

Friedrich, M., Gumbel, J., and Pilgram, R.: Atomic oxygen in the mesosphere and its relevance for the ionosphere, Proc. 14th ESA/PAC Symposium on European Rocket and Balloon Programmes and related research (ESA SP-437, pp. 287–290), Potsdam, Germany, 31 May–3 June 1999.

Greer, R. G. H., Murtagh, D. P., McDade, I. C., Dickinson, P. H. G., Thomas, L., Jenkins, D. B., Stegman, J., Llewellyn, E, J., Witt, G., Mackinnon, D. J., and Williams, E. R.: ETON 1: a database pertinent to the study of energy transfer in the oxygen nightglow, Planet. Space Sci., 34, 771–788, 1986.

Greer, R. G. H., Murtagh, D. P., McDade, I. C., Llewellyn, E. J., and Witt, G.: Rocket photometry and the lower-thermospheric oxygen nightglow, Phil. Trans. R. Soc. Lond. A, 323, 579–595, 1987.

Gumbel, J.: On the accuracy of rocket-borne atomic oxygen measurements, Proc. 25th Annual European Meeting on Upper Atmospheric Studies by Optical Methods, Granada, Spain, 21–25 September, 1998, pp. 25–30, 1999.

Gumbel, J. and Witt, G.: Monte Carlo studies of the resonance fluorescence technique for atmospheric oxygen measurements, J. Quant. Spectrosc. Radiat. Transf., 58, 1–17, 1997.

Gumbel, J., Murtagh, D. P., Witt, G., Espy, P. J., and Schmidlin, F. J.: Odd oxygen measurements during the NLC-93 rocket campaign, J. Geophys. Res., 103, 23399–23414, 1998.

Hedin, A. E.: Extension of the MSIS thermosphere model into the middle and lower atmosphere, J. Geophys. Res., 96, 1159–1172, 1991.

Heppner, J. P. and Meridith, L. H.: Nightglow emission altitudes from rocket measurements, J. Geophys. Res., 63, 51–65, 1958.

Jacobsen, T. A. and Friedrich, M.: Electron density measurements in the lower *D*-region, J. Atmos. Terr. Phys., 41, 1195–1200, 1979.

Jenkins, D. B., Watkin, G., Wareing, D. P., Freeman, G. H. C., Dickinson, P. H. G., and Mackinnon, D. J.: Resolved line profiles of atomic oxygen resonance lamps used in the upper atmosphere, J. Quant. Spectrosc. Radiat. Transf., 34, 123–132, 1985.

Lübken, F.-J., Rapp, M., Siebert, J., and Fricke, K.-H.: The thermal and dynamical state of the upper atmosphere during the first flight of the NLTE campaign, Proc. 14th ESA/PAC Symposium on European Rocket and Balloon Programmes and related research (ESA SP-437, pp. 363–368), Potsdam, Germany, 31 May–3 June 1999.

Martin, L. R., Cohen, R. B., and Schatz, J. F.: Quenching of laser induced fluorescence of $O_2(b^1\Sigma_g^+)$ by O_2 and N_2, Chem. Phys. Lett., 41, 394–396, 1976.

McDade, I. C., Llewellyn, E. J., Greer, R. G. H., and Witt, G.: Altitude dependence of the vibrational distribution of $O_2(c^1\Sigma_u^-)$ in the nightglow and the possible effects of vibrational excitation in the formation of $O(^1S)$, Can. J. Phys., 62, 780–788, 1984.

McDade, I. C., Murtagh, D. P., Greer, R. G. H., Dickinson, P. H. G., Witt, G., Stegman, J., Llewellyn, E. J., Thomas, L., and Jenkins, D. B.: ETON 2: Quenching parameters for the proposed precursor of $O_2(b^1\Sigma_g^+)$ and $O(^1S)$ in the terrestrial nightglow, Planet. Space Sci., 34, 789–800, 1986a.

McDade, I. C., Llewellyn, E. J., Greer, R. G. H., and Murtagh, D. P.: ETON 3: Altitude profiles

of the nightglow continuum at green and near infrared wavelengths, Planet. Space Sci., 34, 801–810, 1986b.
McDade, I. C., Llewellyn, E. J., Murtagh, D. P., and Greer, R. G. H.: ETON 5: Simultaneous rocket measurements of the OH Meinel $\Delta\upsilon$=2 sequence and (8,3) band emission profiles in the nightglow, Planet. Space Sci., 35, 1137–1147, 1987a.
McDade, I. C., Llewellyn, E. J., Greer, R. G. H., and Murtagh, D. P.: ETON 6: A rocket measurement of the O_2 infrared atmospheric (0-0) band in the nightglow, Planet. Space Sci., 35, 1541–1552, 1987b.
Meriwether Jr., J. W.: A review of the photochemistry of selected nightglow emissions from the mesopause, J. Geophys. Res., 94(D12), 14629–14646, 1989.
Mlynczak, M. G., Solomon, S., and Zaras, D. S.: An updated model for $O_2(a^1\Delta_g)$ concentrations in the mesosphere and lower thermosphere and implications for remote sensing of ozone at 1.27 µm, J. Geophys. Res., 98(D10), 18639–18648, 1993.
Mlynczak, M. G., Morgan, F., Yee, J.-H., Espy, P., Murtagh, D., Marshall, B., and Schmidlin, F.: Simultaneous measurements of the $O_2(^1\Delta)$ and $O_2(^1\Sigma)$ airglows and ozone in the daytime mesosphere, Geophys. Res. Lett., 28, 999–1002, 2001.
Murtagh, D. P., McDade, I. C., Greer, R. G. H., Stegman, J., Witt, G., and Llewellyn, E. J.: ETON 4: An experimental investigation of the altitude dependence of the $O_2(A^3\Sigma_u^+)$ vibrational populations in the nightglow, Planet. Space Sci., 34(9), 811–817, 1986.
Murtagh, D. P.: A self-consistent model of the most common nightglow emissions, Proc. Ninth ESA/PAC Symposium on European Rocket and Balloon Programmes and related research (ESA SP-291), Lahnstein, Germany, 3–7 April 1989.
Murtagh, D. P., Witt, G., Stegman, J., McDade, I. C., Llewellyn, E. J., Harris, F., and Greer, R. G. H.: An assessment of proposed $O(^1S)$ and $O_2(b^1\Sigma_g^+)$ nightglow excitation parameters, Planet. Space Sci., 38(1), 45–53, 1990.
Offermann, D., Friedrich, V., Ross, P., and von Zahn, U.: Neutral gas composition measurements between 80 and 120 km, Planet. Space Sci., 29, 747–764, 1981.
Rapp, M., Gumbel, J., and Lübken, F.-J.: Absolute density measurements in the middle atmosphere, Ann. Geophys., 19, 571–580, 2001, http://www.ann-geophys.net/19/571/2001/.
Rauthe, M., Gerding, M., and Lübken, F.-J.: Seasonal changes in gravity wave activity measured by lidars at mid-latitudes, Atmos. Chem. Phys., 8, 6775–6787, 2008, http://www.atmos-chem-phys.net/8/6775/2008/.

Rawlins, W. T. and Kaufman, F.: Characteristics of O(I) and N(I) resonance line broadening in low pressure helium discharge lamps, J. Quant. Spectrosc. Radiat. Transfer, 18, 561–572, 1977.

Rees, D. and Fuller-Rowell, T. J.: Understanding the transport of atomic oxygen within the thermosphere, using a numerical global thermospheric model, Planet. Space Sci., 94, 935–948, 1988.

Russell, J. P., Ward, W. E., Lowe, R. P., Roble, R. G., Shepherd, G. G., and Solheim, B.: Atomic oxygen profiles (80 to 115 km) derived from Wind Imaging Interferometer//Upper Atmospheric Research Satellite measurements of the hydroxyl and greenline airglow: Local time–latitude dependence, J. Geophys. Res., 110, D15305, doi:10.1029/2004JD005570, 2005.

Sharp, W. E.: Absolute concentrations of O(^3P) in the lower thermosphere at night, Geophys. Res. Lett., 7, 485–488, 1980.

Sharp, W. E.: The measurement of atomic oxygen in the mesosphere and lower thermosphere, Planet. Space Sci., 39, 617–626, 1991.

Shepherd, G. G., Liu, G., and Roble, R. G.: Large-scale circulation of atomic oxygen in the upper mesosphere and lower thermosphere, Adv. Space Res., 35, 1945–1950, 2005.

Slanger, T. G. and Black, G.: Interactions of $O_2(b^1\Sigma_g^+)$ with O(^3P) and O_3, J. Chem. Phys., 70, 3434–3438, 1979.

Slanger, T. G. and Copeland, R. A.: Energetic oxygen in the upper atmosphere and the laboratory, Chem. Rev., 103, 4731–4766, 2003.

Stegman, J., Llewellyn, E. J., Dickinson, P. H. G., and Jenkins, D. B.: On the triplet states of molecularoxygen in the upper atmosphere, Proc. of the 10th Annual Meeting on Upper Atmospheric Studies by Optical Methods, Grasse, France, September 6–11, 1982, edited by: Clairemidi, J., Observatoire de Besançon, Université de Besançon, pp. 243–251, 1983.

Stegman, J. and Murtagh, D. P.: The molecular oxygen band systems in the UV nightglow: measured and modelled, Planet. Space Sci., 39(4), 595–609, 1991.

Thomas, R. J.: Analysis of atomic oxygen, the green line and Herzberg bands in the lower thermosphere, J. Geophys. Res., 86, 206–210, 1981.

Ulwick, J. C., Ratkowski, A. J., and Makhlouf, O.: Twilight rocket measurements of high-latitude atomic oxygen density during the DYANA campaign, J. Atmos. Terr. Phys., 56, 1871–1883, 1994.

Vallance Jones, A.: Aurora, D. Reidel Publishing Company, Dordrecht, 1974.

Wayne, R. P.: Chemistry of Atmospheres (3rd edition), Oxford University Press, Oxford, 2000.
Witt, G., Stegman, J., Murtagh, D. P., McDade, I. C., Greer, R. G. H., Dickinson, P. H. G., and Jenkins, D. B.: Collision energy transfer and the excitation of $O_2(b^1\Sigma_g^+)$ in the atmosphere, J. Photochem., 25, 365–378, 1984.
Young, R. A.: Measurement of the atomic concentration in planetary atmospheres, Proposal for Research No. 61-202, Stanford Research Institute, Menlo Park, California, 1961.

Table 1. Adopted rate coefficients and excitation parameters. All coefficients are in molecule cm^3 second units. T is the atmospheric temperature.

Coeff.	Value	Reference
k_1	$4.7\times10^{-33}(300/T)^2$	Campbell and Gray (1973)
$k_2^{O_2}$	4.0×10^{-17}	Martin et al. (1976)
$k_2^{N_2}$	2.2×10^{-15}	Martin et al. (1976)
k_2^{O}	8.0×10^{-14}	Slanger and Black (1979)
k_2^{O}	0	McDade et al. (1986a)
k_3^{O}	$2.4\times10^{-10}\cdot\gamma$	Stegman and Murtagh (1991)
$k_3^{O_2}$	$9.8\times10^{-11}\cdot\gamma$	Stegman and Murtagh (1991)
A_1	0.079	Vallance Jones (1974)
A_2	0.083	Vallance Jones (1974)
A_3	0.85	Stegman and Murtagh (1991)
Excitation parameters for use with $k_2^{O}=8\times10^{-14}$:		
C^{O_2}	6.6±0.4	McDade et al. (1986a)
C^{O}	19±2	McDade et al. (1986a)
Excitation parameters for use with $k_2^{O}=0$:		
C^{O_2}	7.5±0.5	McDade et al. (1986a)
C^{O}	33±4	McDade et al. (1986a)

AMTD
2, 1419–1452, 2009

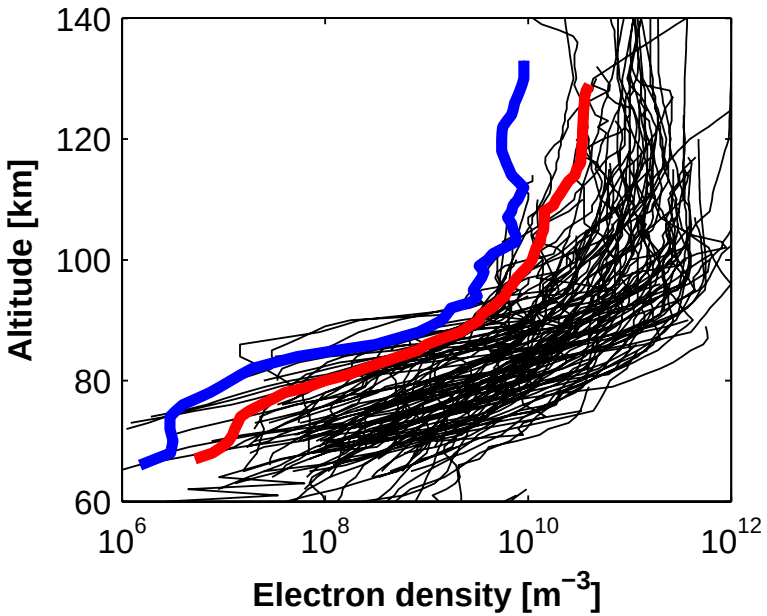

Fig. 1. Electron density measurements from NLTE-1 (red profile) and NLTE-2 (blue profile) together with other measurements north of 60° N latitude (thin black profiles) (M. Friedrich, private communication).

AMTD
2, 1419–1452, 2009

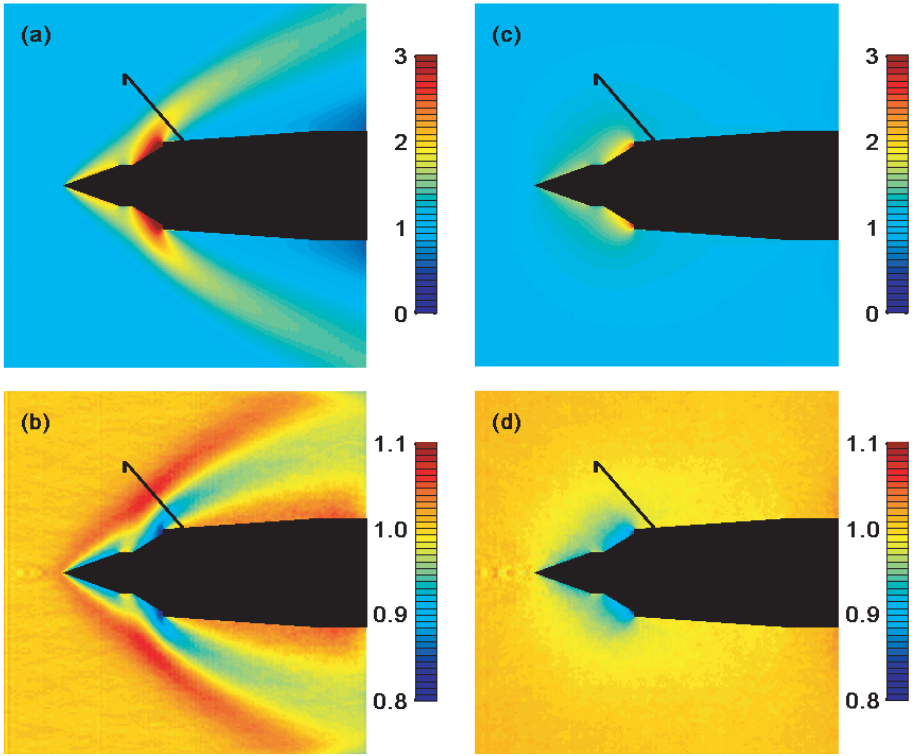

Fig. 2. Direct Simulation Monte Carlo simulation of the interaction between the NLTE rocket payload and the surrounding atmosphere. Panel **(a)** shows the total air density normalised with the unperturbed air density, and panel **(b)** shows the normalised O mixing ratio, both at 90 km altitude. Panel **(c)** and **(d)** shows the same properties as (a) and (b) but for 120 km altitude. The boom is not included in the flow simulations.

AMTD
2, 1419–1452, 2009

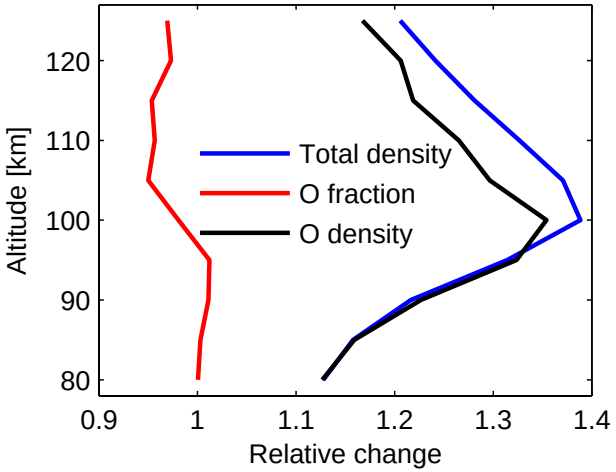

Fig. 3. Aerodynamic simulation of the interaction of the NLTE rocket payload with the atmosphere and the effect on the total air density and O mixing ratio at different altitudes. The profiles show the relative change in the absorption path between the lamp and the absorption experiment on the boom.

AMTD
2, 1419–1452, 2009

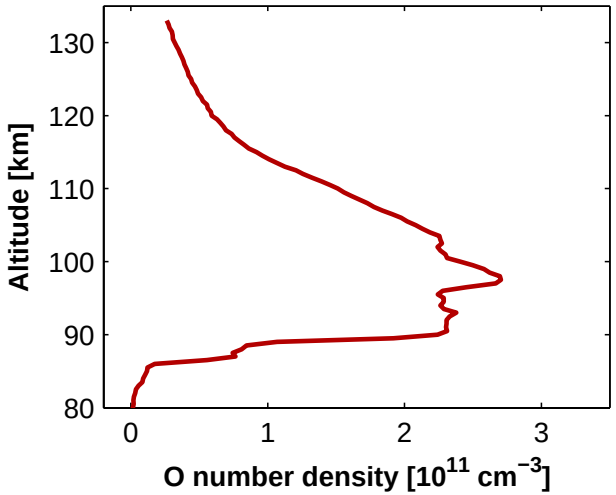

Fig. 4. The atomic oxygen number density measured with the resonance fluorescence and absorption technique during the NLTE-2 rocket launch.

AMTD
2, 1419–1452, 2009

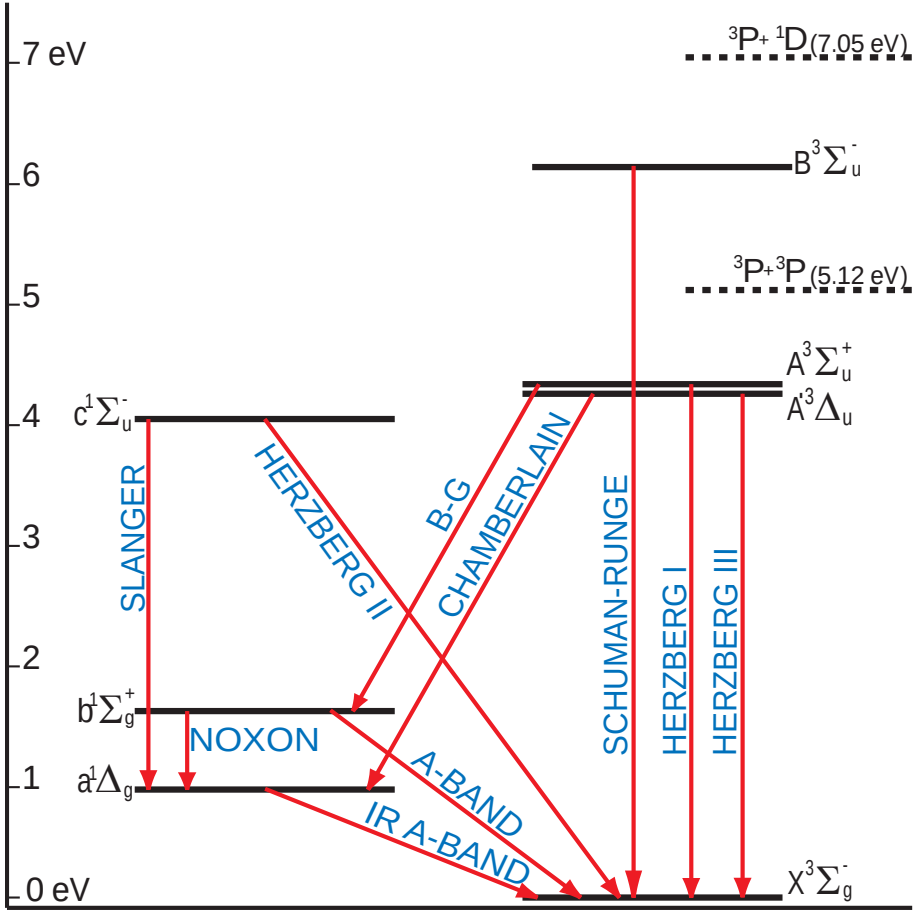

Fig. 5. Energy level diagram of O_2 transitions in the nightglow (after Greer et al., 1987).

AMTD
2, 1419–1452, 2009

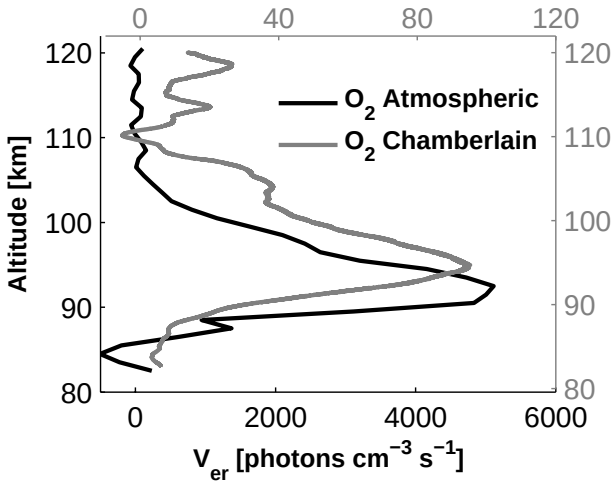

Fig. 6. Measured nightglow profiles during the NLTE-2 rocket launch. Volume emission rate of the (0-0) $O_2(b^1\Sigma)$ atmospheric band at 762 nm (black line) and (5-3) band of the $O_2(A'^3\Delta)$ Chamberlain system at 391 nm (gray line).

AMTD
2, 1419–1452, 2009

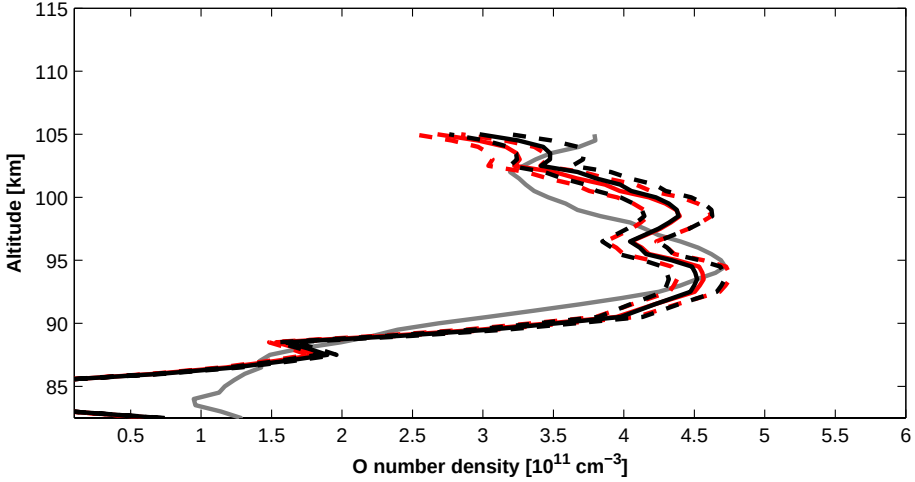

Fig. 7. Atomic oxygen number density derived from the nightglow measurements during NLTE-2. The gray line is the inverted Chamberlain nightglow emission profile. The solid red and black lines are the inverted atmospheric band emission profiles with and without quenching of the precursor state by atomic oxygen, respectively. The dashed red and black lines show the possible error due to uncertainties in the rate constants for the atmospheric band inversion.

AMTD
2, 1419–1452, 2009

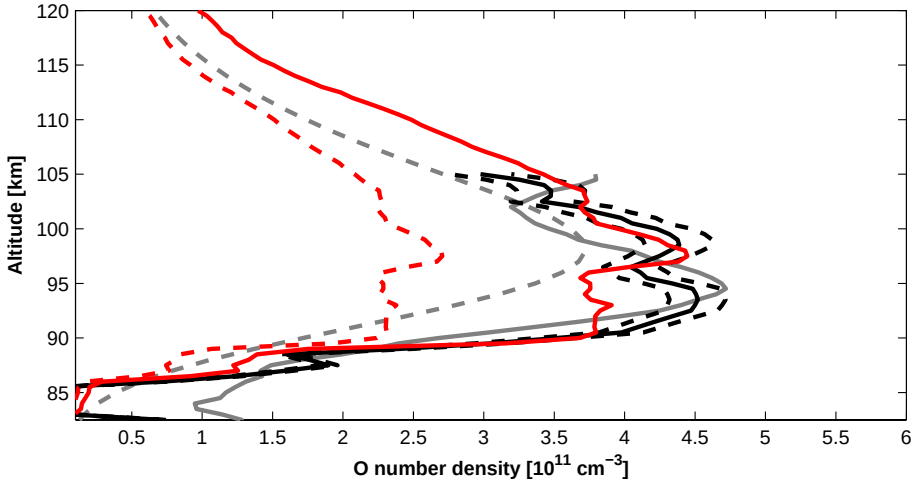

Fig. 8. The solid gray line and the black lines as in Fig. 7. The dashed red line is the measured atomic oxygen profile from the direct technique from Fig. 4. The solid red line is the nightglow-calibrated direct measurement and the dashed gray line is the MSIS-E90 atomic oxygen profile from the time of the NLTE-2 launch.

AMTD
2, 1419–1452, 2009

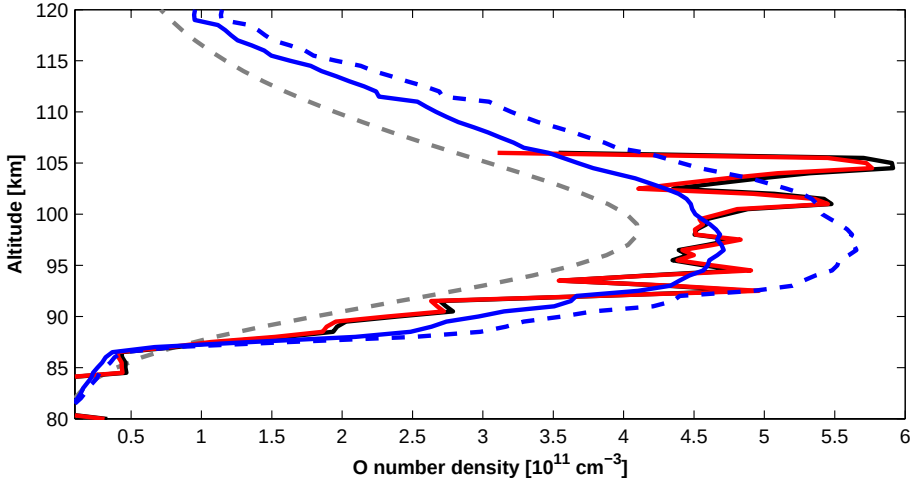

Fig. 9. Atomic oxygen profiles from NLTE-1. The red and black lines show the inverted atmospheric band emission with and without quenching of the precursor state by atomic oxygen, respectively. The dashed blue line is the measured atomic oxygen profile from the direct technique. The solid blue line is the nightglow-calibrated direct measurement and the dashed gray line is the MSIS-E90 atomic oxygen profile from the time of the NLTE-1 launch.

AMTD
2, 1419–1452, 2009

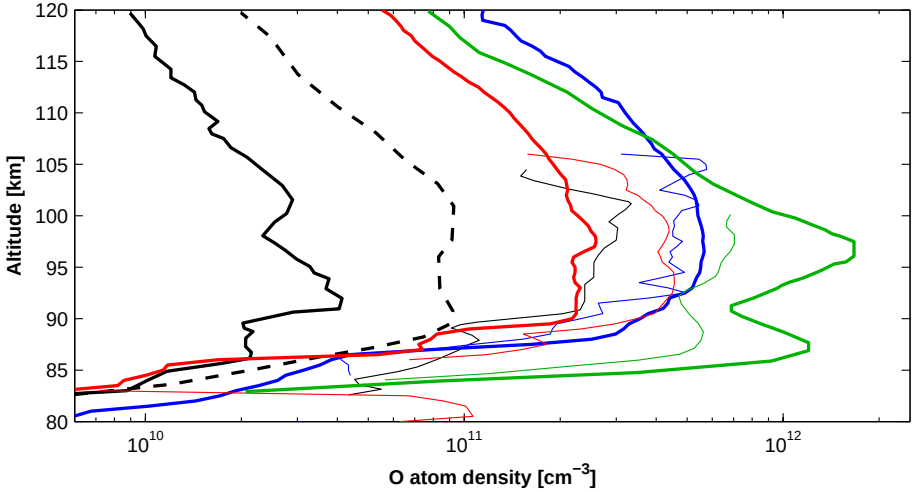

Fig. 10. Comparison between the NLTE results and other earlier measurements. Heavy lines denote atomic oxygen profiles obtained from direct measurements while thin lines denote oxygen profiles obtained from O_2 atmospheric band inversions. The black lines are from SOAP/WINE (solid thick and thin lines) and USU (dashed line, 72 min after SOAP, resonance fluorescence only); the blue lines are the profiles from NLTE-1 (without nightglow calibration); red lines are the profiles from NLTE-2 (again without nightglow calibration); and the green lines are the profiles obtained during the OXYGEN/S35 sounding rocket campaign. Note the spread by a factor of 50 in the direct measurements and only by a factor of 3 in the profiles from the nightglow inversion.

AMTD
2, 1419–1452, 2009

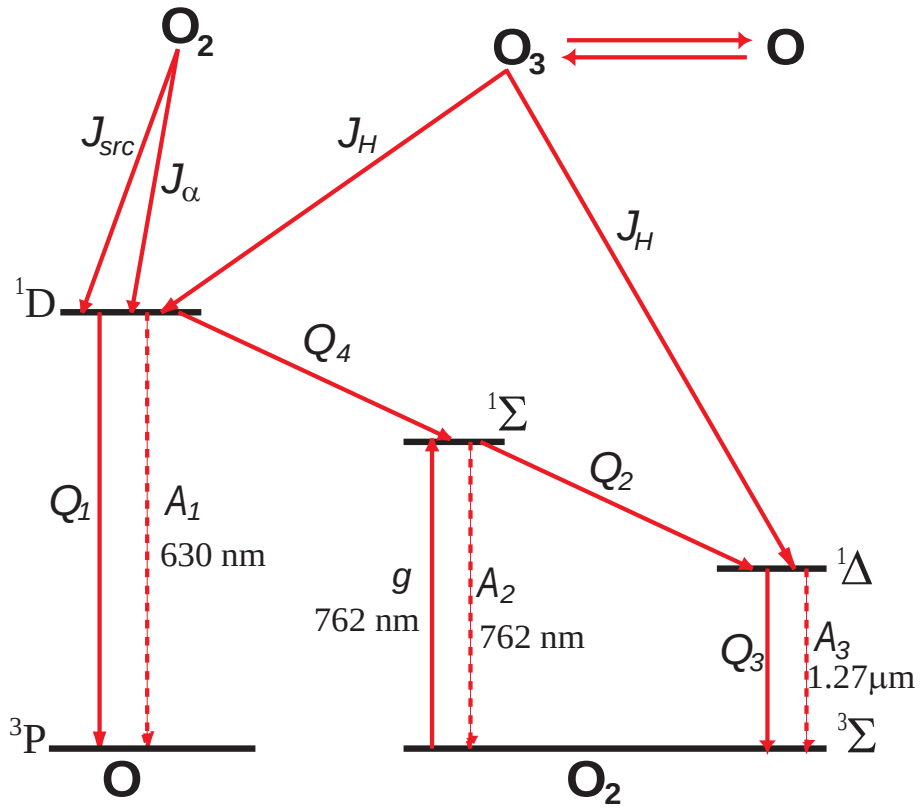

Fig. 11. The $O_2(a^1\Delta_g)$ dayglow production mechanisms (after Mlynczak et al., 1993). *J* indicate solar photolysis, *Q* collisional quenching, *A* spontaneous emission, and *g* solar absorption in the atmospheric band.

AMTD
2, 1419–1452, 2009